Lessons Learned from Level 3 Analyses on Bending Strain Features

Rhett Dotson[1], Jeff Haferd[2], Karim Kabbara[2], Nic Roniger[2]
[1]D2 Integrity, LLC, [2]Marathon Petroleum

Pipeline Pigging and Integrity Management Conference

February 12-16, 2024

Organized by
Clarion Technical Conferences

https://doi.org/10.52202/072781-0012

https://doi.org/10.52202/072781-0012

Abstract

The use of bending strain analyses for identifying and managing pipeline geohazards has grown significantly in the last decade. While bending strain assessments are useful for identifying and prioritizing geohazard features impacting pipelines, it is understood that bending strain assessments cannot provide the total strain which is required for comparison to calculated tensile or compressive strain capacities in determining fitness for service. The inability to easily calculate membrane strain and the resulting total strain in impacted pipelines represents a gap in the industry. A few simplified methodologies have been proposed to estimate the membrane strain based on the displaced shape of the pipeline, and some ILI technologies are available for explicitly measuring the membrane strains. Level 3 numerical analysis is another method that can be used to estimate the membrane, bending, and total strain states in a pipeline impacted by a geohazard. This paper presents the results of a study covering nine finite element analyses completed on separate geohazards with varying characteristics. The paper discusses the methods used in the study to construct the models, including incorporating initial strains and estimating as-built conditions of the pipeline. Comparisons are provided between the membrane strains calculated explicitly in the models and membrane strains estimated using simplified methods. The study examines how membrane and bending strains develop and progress at larger pipeline displacements noting important differences in axially and laterally oriented geohazards. The conclusions from this study provide useful insights to operators on how to perform level 3 geohazard assessments, and how to properly use the results to make informed integrity management decisions for monitoring or mitigation of geohazards threats.

Background

The awareness of geohazards among operators and regulators in the United States has grown significantly in the last decade. The management of geohazards relies primarily on data gathered from in-line inspections equipped with inertial measurement units (IMU) or surface-based assessments utilizing LiDAR or publicly available information. While both methods are useful for identifying geohazards, bending strain assessments based on IMU provide the most straightforward information for quantifying the severity and influence of the features on the pipeline, thereby permitting proper sentencing. Many approaches to geohazard integrity management rely on the magnitude and orientation of the bending strain when sentencing features [1, 2].

It is understood that the bending strain calculated based on IMU represents only a portion of the total axial strain in the pipeline. The membrane strain component results from the uniform axial stretching or compression of the pipe. During most normal pipeline operations, the axial membrane strain in a pipeline is insignificant as pipeline design is usually controlled by the hoop stress, particularly for buried pipelines. However, when a pipeline is displaced from its as-laid condition, as occurs in geohazards, the membrane strains become larger and can represent a significant portion of the total axial strain. This fact becomes important because calculations for tensile strain capacity in girth welds or compressive strain capacity in the pipe body are based on the total axial strain in the pipeline rather than only the bending strain. However, most operators compare calculated bending strains to these limits as the total axial strain cannot be easily calculated.

The industry has proposed both analytical and ILI-based solutions for quantifying the membrane strain. A 2020 IPC paper by Fathi and others [3] proposed a method for estimating membrane strains based on the calculated span length and horizontal deflection. The method was based on parametric finite element models with various soils and displacement profiles. This publication provides a useful

https://doi.org/10.52202/072781-0012

tool for simplified shapes. However, broad application of the method is difficult for complex profiles or movement that has both horizontal and vertical components. ILI-based solutions using the magnetic response of the steel material have also entered the market in the last decade [4]. The use and accuracy of these technologies is still being evaluated by operators. Key questions surround the material data required to get accurate estimates of the strain and the ability to accurately quantify membrane strains greater than the plastic limit (typically 0.2%).

The authors of this paper identified nine sites that had various levels of bending strain and responses ranging from on-site monitoring to stress relief or even pipe replacement. Detailed numerical models were constructed at each of the sites to calculate the total strain in the pipeline based on current conditions and estimate the response of the pipelines under simulated future movement. The results from these analyses were compared to the analytical estimations of membrane strain and used to ensure adequate response margins for future movement. This paper discusses the methods and lessons learned from these analyses.

Case Study Data

The nine sites selected for the case study are presented in **Table 1**. The sites cover a range of pipe sizes from NPS 8 to NPS 24 with varying geohazard orientations. Feature #3 in the table was not a reported bending strain feature; instead, the feature was identified during a surface-based assessment. The reported bending strains for the features ranged from 0.09% to 0.684%. Stress relief operations had been performed at six of the locations, and the impacts of the stress relief were accounted for in the analysis. Six of the sites had strain gages installed, and guidance was provided on alarm limits for these locations.

Methodology

The process for assessing each of the sites is shown graphically in **Figure *1*** and described herein. The process begins with a review of the bending strains for each site. The purpose of this review is to ensure that the extents of the bending strain feature adequately capture the influence of any suspected geohazard. The review of the bending strains also examines the navigation heading angles to identify patterns that are consistent with external loads.

The second step involves recreating the as-built shape of the pipeline. It is important to note that recreating the as-built location is only required when a baseline IMU data set acquired near the time of construction is not available. This is common for pipelines constructed prior to 2000. However, if operators acquire baseline IMU data near the time of construction, it reduces the uncertainty in the analysis. The second step is performed by reviewing the shape of the pipeline, the geohazard orientation, and the heading angles from the IMU. While the vertical profile of a pipeline may continuously change, the horizontal orientation of a pipeline is typically "near" straight. When reviewing an area impacted by a geohazard, the azimuth heading angle upstream and downstream of the geohazard can provide an indication of the original trajectory. An example of this is shown in **Figure 2** for site #7. IMU data sets from 2018 and 2022 were available at this location and showed a clear progression in the deviation of the azimuth due to a geohazard acting on the pipeline. Additionally, the azimuth measures 272 degrees immediately upstream and downstream of the deviation. This permits the heading angle to be reconstructed and pipeline coordinates to be regenerated from the simulated heading angle. While this example shows a single linear trajectory, a similar process using multi-linear projections is also possible. This process may also be used for

https://doi.org/10.52202/072781-0012

reconstructing the pitch angle at locations where vertical deviation is observed. However, identifying a clear original orientation in the pitch is usually more challenging.

The finite element models can be built once the as-built pipeline location has been generated. The finite element models are assessed using the general-purpose finite element code Abaqus. The pipeline is modelled using 3-D pipe elements (PIPE31). The material properties for the pipeline are based on specified minimum properties from API 5L and a Ramberg-Osgood formulation for the stress strain curve. The influence of the soil is modelled using the built-in pipe-soil interaction elements (PSI34) which are based on elastic-plastic multi-linear spring formulations from the ALA document [5]. Soil properties and depth of cover are based on field measurements when available. If in-situ soil properties were not available for a site, then soil properties were based on a 3-ft cover depth and an "average" clay material having a shear strength of 50 kPa. The soil properties for stress relief excavations used user-specified soil properties for the axial and horizontal stiffness based on the weight of the pipe and a friction coefficient of 0.3. The vertical soil properties were specified as negligible in the vertical uplift direction and unchanged in the vertical downward direction. Some of the stress relief operations utilized a non-native backfill. The properties for these soils were based on a sand formulation with a bulk unit weight of 125 pcf and a shear angle of 0.25.

Loads are applied to the Abaqus model in a sequential matter with non-linear formulations. The steps described in this section require the use of the model change option in Abaqus to remove and reactivate portions of the soils and pipeline to simulate the in-place strains and stress relief operations. The in-place strains were simulated using translational displacements applied to an initially straight pipeline segment to match the recreated pipe position. This methodology effectively replicates the in-place bending strains without inducing significant membrane strains. Next, boundary conditions are applied to the soil nodes to displace the pipeline. The displacements are calibrated to match the shape of the pipeline as captured by the most recent IMU. Next, if applicable, stress relief operations are simulated by removing the displaced in-situ soil and replacing that soil with excavated properties. After simulating the relief operations, the soil properties are switched again. If non-native soils were used in the trench, then appropriate replaced soil properties were specified for future movement. Future movement was simulated in the last analysis step. Future movement was simulated by scaling the calibrated profile without increasing the extents. This assumes that the landslide does not change width or orientation as future movement occurs.

Key Performance Indicators (KPIs) were extracted from the models after completing the assessment. At the highest level, the analysis would answer the question how much pipe movement can be sustained before an assumed or calculated tensile strain capacity (TSC) is exceeded at a girth weld or the compressive strain capacity (CSC) is exceeded in the pipe body. This information is useful for locations where site surveys or geodetic monuments are avaialble to monitor movement. In locations where strain gages are placed, the results can be used to relate the measured strains to the peak strains from the analysis.

Results

This results section summarizes the lessons learned from the numerical analysis and general trends observed in the analyses. The first learning came from the review of the calculated bending strains and the reported bending strain features. This review, while appearing as a cursory step in the process, often revealed that bending strain features were identified too short and did not capture the full extents of the geohazard feature or accurately depict the displaced condition of the pipeline. For example, the reported horizontal strains and out-of-straightness for site #6 are reproduced in **Figure**

https://doi.org/10.52202/072781-0012

3. The image shown in **Figure *3*** has been recreated in D2I's Atlas software to avoid identifying the original vendor who reported the feature. Additionally, in the interest of brevity, only the horizontal information is shown for the bending strain feature at Site #6. Site #6 was reported with a length of 194 ft and what appears to be a 0.9-ft lobe with the pipeline deviating to the right as measured by the direction of flow. Stress relief operations were planned for Site #6, and the pipeline was expected to rebound in the direction shown by the yellow arrows in **Figure *3***. However, during the stress relief operations, the upstream portion of the pipeline was observed to move in the opposite direction as indicated by the blue arrows.

The assessment for Site #6 occurred after the stress relief excavations were completed and the unexpected movement was observed. During the review of the bending strains, it was identified that the original reported bending strain feature was too short and did not capture the entire displaced profile. The horizontal information is shown again in **Figure *4*** but the viewable extents of the strain area are increased upstream and downstream. When the viewable extents of the strain area are increased, a second upstream lobe can be clearly seen with a matching rightward/downslope horizontal strain pattern. The hypothetical as-built centerline is annotated on the figure to show the two lobes. In addition, the cause of the movement observed during stress relief operations becomes clear. The section of pipeline between the two lobes displaced to a position more in-line with the lobes on either side. These findings also aligned with the observed geomorphic review at site #6 which identified landslide interaction with the pipeline upstream of the original bending strain feature. The review of site #6 suggested that the actual length of the feature was 356 feet rather than the originally reported 194 feet.

Similar occurrences of overly short bending strain features were observed at site #1 and site #9. The reported horizontal strains and out of straightness are reproduced for site #9 in **Figure *5***. This feature was reported as 247-ft long and was interpreted as having a right-ward displaced lobe as annotated by the yellow arrows in the figure. Although this feature interacted with a mapped landslide, the orientation of the displacement appeared opposite the direction of the identified slope movement. However, when the viewable extents of the feature were increased, it revealed two lobes with displacements in the direction of the mapped landslide as shown in **Figure *6***. After the review, the length of the feature was increased to 398-ft. This example clearly demonstrates how the viewable extents of horizontal features can impact the out-of-straightness and resulting interpretation of the pipe deformation.

Site #1 provides the final example from the strain review. Site #1 was reported as two separate strain features having lengths of 169-ft and 274-ft with out-of-straightness of 2-ft and 7-ft, respectively, as annotated in **Figure *7***. However, after a review of the bending strain features, the two were combined and the site was increased to 450ft with an offset of 9-ft, as annotated in **Figure *7***. The discrepancy was caused by the fact that the middle portion of the landslide did not have high bending strains. However, a larger view of the out-of-straightness and the heading angles confirmed a larger displaced shape that matched observations from the field.

The analysis results showed similar behaviour based on landslide orientation. Therefore, a few of the results are chosen to demonstrate the trends and lessons learned for each orientation. Site #5 illustrates the typical behavior of a lateral landslide. The strain results for the calibrated model, including the membrane and total strain, are shown in **Figure 8**. The top five panels compare the results between the IMU, shown as a solid line, and the FEA, shown as a dashed line. The membrane strain and the total strain are shown in the sixth and seventh vertical panels, respectively. At the point of calibration to the IMU data, the maximum combined bending strain is 0.435% which is very near

https://doi.org/10.52202/072781-0012

the reported combined strain of 0.45%. At this same point, the maximum membrane strain is 0.37% and the total strain is 0.801%. This is significant because in this scenario the bending strain represents only half of the total strain and would be unconservative if used for integrity decisions. When the reported length and out-of-straightness were combined with the methodology from [3], the membrane strain was estimated as 0.19%. The underestimation of the membrane strain may be because the membrane strains do not distribute uniformly as shown in **Figure *8***.

The progression of the strain profiles for Site #5 is shown in **Figure 9**. The soil displacements were incrementally increased up to three times the baseline displacement producing a total horizontal movement of 21-feet. It is interesting to note that the membrane strains increase more rapidly at larger displacements and become greater than the bending strains after 8-ft of movement. In addition, the maximum membrane strains are not coincidentally located with the peak bending strains. Instead, the membrane strains are a maximum in the displaced portions between the toes and the crest of the movement area. This results in the maximum overall strain location shifting to the locations annotated as dashed red lines in **Figure 9**. The maximum strain values independent of location are plotted as a function of pipe displacement in **Figure 10**. These results show the influence of simulated stress relief and landslide progression. The strain progression curves show that the maximum membrane strain begins accumulating at a faster rate than the bending strain between 7 and 10-ft of movement. The other evaluated sites showed similar behaviour with regards to the membrane strains rapidly increasing at larger movement. In some cases, the bending strains were also observed to plateau as shown in **Figure 11** for Site #2.

The results in **Figure *10*** and **Figure *11*** provide two important observations pertinent to horizontal landslides. First, the membrane strains progress rapidly at larger pipe displacements and become more significant than the bending strains in the total strain. If the reported bending strains are the only basis for integrity calculations in pipelines with larger displacements this can lead to results that are unconservative. Second, the peak bending strains may not continue to increase at larger displacements and should not be relied upon as a sole indicator of stability in pipelines with larger displacements. In other words, if the response to a landslide is being determined by examining only the maximum reported bending strain between inspections, this can lead to a false sense of security for pipelines with larger displacements. “Larger” pipe displacements may conservatively be assumed as 4-5 feet based on the observations from these assessments. It is also noteworthy that the compressive strains did not control for any of the lateral landslides that were analyzed. This is primarily due to the large tensile membrane strains present in horizontal landslides.

The strain response for an axially oriented landslide is distinctly different from the horizontal landslide. First, the bending strains do not change significantly in the early stages of landslide movement. Additionally, the membrane strains do not exhibit uniform tension or compression. Instead, the membrane strains exhibit tension near the head of the landslide where the pipeline is “stretched” and compression near the toe of the landslide where the pipeline is “pinched”. This variation in strain is shown graphically in **Figure *12*** for site #3, and similar results were observed for site #4. At both sites, the analysis did not show significant changes in the out-of-straightness or the bending strain as the landslide progressed. Additionally, the critical limits were controlled by the compressive strain capacity near the toe of the landslide for both sites as shown in **Figure 13** for site #3. These findings confirm that the use of bending strain alone for the management of axially oriented landslides is challenging and may not be able to identify landslide features before they are at risk for developing buckles.

https://doi.org/10.52202/072781-0012

In addition to the strain progression observed in the models, the membrane strains were compared to the results from the analytical solutions in [3]. The results of the comparison are shown in **Table 2**. The analytical solutions were developed based on models of simple, single lobe landslides with a conventional bell shape. The analytical calculations used for the comparison were performed using three points based on the reported length and maximum out-of-straightness in the bending strain reports. The largest discrepancies occurred for sites 1, 5, and 8, and the analytical calculations underpredicted the strains at each site. Sites 1 and 8 do not have simple shapes which suggests that the method should not be used for complex shapes or those that do not have a simple bell-shape. The membrane strain was under-predicted for site #5 as well. This could be due to the larger displacements at site #5 (7-ft), but it is difficult to draw conclusions based on the small data set. It is also worth noting that using the reported lengths with the calculations from [3] would be impacted by features identified with incorrect lengths. These results suggest that the application of results using the methodology in [3] should not rely on reported dimensions but should consider information based on a review of the out-of-straightness plots.

Applications

In addition to the observations regarding the general behaviour of lateral and axial landslides, the results from the level three analysis have immediate application to integrity management decisions. The first application is complimentary to the installation of strain gages. The previous results shown for Site #5 in **Figure 8** illustrate the benefits of the analysis. Site #5 did not have strain gages installed prior to the analysis. Based on the results of the bending strain data alone, the strain gages might have been placed near the peaks of the bending strain at odometers 623900, 624000, and 624050. However, the location of the maximum overall strain and maximum membrane strain occur near odometer 623926 and 624025 suggesting these locations are better suited for capturing the maximum total strain response of the landslide at larger displacements.

In addition to gage placement, the results of the assessment can be used to develop appropriate responses based on the gage readings. The maximum strains from the analysis should not be directly used to determine response. At a minimum, the odometer location of the gages and the circumferential orientation of the gages need to be considered to predict the strain response at the gage location. An example of this is shown in **Figure 14** for Site #2. The predicted maximum strain from the analysis is shown with the solid black line while the predicted response of the strain gages are shown with dashed lines. The maximum strain is consistently higher than the expected strains at the gage locations. Additionally, the future gage responses do not show a linear correlation with the maximum strain at any of the gage locations. For instance, gage #4 is not expected to show significant strain increases until the pipe displacements exceed 10-ft, at which point the strains will increase faster than the overall maximum strain at this location. Similarly, gages 2 and 3 both increase at approximately the same rate as the overall maximum strain until nearly 11 to 12 feet of movement at which point the values will plateau. Understanding this response could be important if gages 2 and 3 are relied upon to judge severity at higher pipeline displacements. In all cases, the maximum overall strain in the system is greater than the values predicted at the gages. Therefore, it is necessary to understand how the gage readings will change as the pipeline movement increases.

The predicted response can also be used to justify limits for strain gages or measured pipe displacements. The strain gage warning limits should vary depending on landslide orientation. For instance, a maximum action limit of 5000 microstrain (0.5%) can be justified at site #2 based on the results in **Figure *14***. Based on the model predictions, this would correlate to an additional 3-ft of pipeline movement and the total strains are predicted to be near 1.1%. However, in practice smaller

https://doi.org/10.52202/072781-0012

values are often chosen for warning limits given the uncertainty associated with geohazards. These limits are typically on the order of 500 – 1000 microstrain (0.05 – 0.1%). These warning limits are larger than the variations expected due to seasonal changes, but small enough to detect subtle changes at the site. When these limits are reached, additional data is collected in the form of updated site visits or an ILI equipped with IMU. The results obtained in these models can help justify that these limits are appropriate and provide safe margins against the ultimate capacity.

While a 5000 microstrain limit may be possible for a lateral landslide, this would not be appropriate for the axial landslide at Site #3. The minimum total strain exceeds 5000 microstrain (0.5%) at 3.6-ft of displacement which is only a 0.6-ft away from when the compressive strain capacity limit is reached. The predicted results also show that even a warning limit of 0.1% would require almost 2-ft of movement. In locations where episodic movement is possible, this margin may be insufficient. However, the behaviour of the membrane strain in axial landslides as observed in the models can be used to improve the warning limits. While strain gages installed across a pipeline would be expected to show uniform increases as a lateral landslide progresses, the opposite behaviour is expected for an axial landslide. For example, gages installed near the head of the landslide should show tensile membrane strains while the gages placed near the toe of the landslide should show compressive membrane strains. This is a because the pipeline is stretched near the head of an axial landslide and pinched near the toe. This information can be coupled with strain gages placed at these locations to define a warning limit that is not based on the strain magnitude from a single gage. Instead, if sets of strain gages are placed near the head and toe of the landslide, then the calculated membrane (i.e., average) strains should be compared between the two sets of gages. If the gages show that the membrane strains are moving in opposite directions, which would not be expected during normal seasonal variations, then it is a strong indicator that the axial landslide is actively impacting the pipeline. This simple comparison would permit the use of lower warning limits and earlier detection.

The results from the strain progression plots are also applicable to develop limits for pipe or soil movement. For instance, in the case of Site #2 in **Figure *11*** or Site #5 in **Figure *10***, the results show that additional pipeline movement up to 2-ft will not result in any of the strain limits being exceeded for either site. This is important because many operators struggle with response to small changes detected from on-site monitoring based on inclinometers or geodetic monuments. While the analysis is based on the movement of the pipe these limits could be applied to geodetic monuments or inclinometers installed at each site.

It is important to recognize the inherent uncertainty that exists in predicting the response of pipelines to active geohazards. Changes in landslide orientation or size could alter the predicted response. In addition, the overall strain progression plots may show that several feet of movement are tolerable; however, in practice a large episodic event could result in several feet of movement that occurs instantly. For this reason, it is important to revisit the results of predictive models once significant changes have been observed at a site. Revisiting the model should examine whether the assumptions for the original model were valid and evaluate the accuracy of the predicted response.

Conclusions

In conclusion, the geohazard threat will continue to receive additional attention and scrutiny in upcoming years. Response measures are expected to include increased usage of in-situ monitoring in the form of strain gages, geodetic monuments, and slope inclinometers. The lessons documented in

https://doi.org/10.52202/072781-0012

this publication are helpful for operators when using these methods coupled with analysis, and they are re-iterated below:

- Sites identified based on bending strain analysis should be reviewed prior to developing a response plan. The strain response and out-of-straightness patterns should be reviewed upstream and downstream of the identified feature to ensure regions impacted by a geohazard were adequately captured.
- For laterally oriented landslides, membrane strains are typically low (<0.1%) for displacements less than 2-3 feet, and the bending strains are the largest portion of the total strain. This permits the use of maximum bending strains values for the management of lateral geohazards with small displacements. For larger displacements, the membrane strains begin increasing rapidly and can become the largest component of the total strain.
- For axially oriented landslides, the bending strains may not be above the reporting threshold or show much change as the landslide progresses initially. However, the membrane strains will show variation between the head and the toe of the landslide, and this information can be coupled to define refined actionable limits for in-situ strain gages.
- The membrane strains can be estimated using reported feature dimensions and the methodology in [3]. However, operators should take care when using the method with complex shapes that do not resemble a single lobe or a bell-shape. Additionally, for larger landslides, the method may not be accurate as membrane strains do not distribute evenly in the displaced pipeline.
- The results of advanced Level 3 analysis can be used to justify or develop warning limits based on pipeline movement or soil movement. However, the limits should be conservatively set and revisited to ensure the analysis assumptions are valid.

References

1. INGAA Foundation, Geosyntec Consultants, Inc. Guidelines for Management of Landslide Hazards for Pipelines, Version 1, August 17 2020.
2. Dotson, R., McKenzie-Johnson, A., How Should we Respond to Geohazards, Pipeline Pigging and Integrity Management Conference, February 6-10, 2023.
3. Fathi, A., Yoosef-Ghodsi N., Ndubuaku, O., Hill, M., Rapid Strain Demand Estimation of Pipelines Deformed by Lateral Ground Movements, IPC 2020-9259.
4. ElSeify, M., In-Line Inspection of Both Axial and Bending Strains, a More Comprehensive Approach to Define Pipeline Strain Conditions, Pipeline Technology Conference 2020.
5. American Lifelines Alliance, Guidelines for the Design of Buried Steel Pipe, February 2005.

https://doi.org/10.52202/072781-0012

Table 1: Particulars of Case Study Sites

Site #	OD	Comb. Bending Strain (%)	Strain Orientation	Current Response[1]	Reported Length (ft)	Feature OOS (ft)
1	16	0.684	Combined	REP, DBF, EHD, SGU, INC	274	7
2	24	0.310	Horizontal	STR, SGU, DBF, GWR, INC, EHD, SST	151	4
3	14	0.090	Axial	STR, GWR, SGU, INC, DBF, EHD, SST	n/a	n/a
4	24	0.307	Axial	STR, GWR, SGU, DBF, EHD	104	2
5	20	0.450	Horizontal	STR, GWR, SGU, INC, DBF, EHD	255	7
6	24	0.260	Horizontal	STR, GWR, SGU, INC, EHD, DBF, SST	112	1.6
7	16	0.220	Horizontal	INC, SST	174	1
8	8.625	0.317	Horizontal	STR, GWR, SGU, DBF, INC, EHD	185	1.5
9	24	0.194	Combined	SST	245	1

Table 2: Membrane Strain Comparison for Horizontal Movement

Site	**Simple Shape?**	**Length (ft)**	**OOS (ft)**	**Membrane Strain from [3]**	**Membrane Strain from Analysis**
1	No	274	7	0.16%	0.86%
2	Yes	151	4	0.17%	0.18%
5	Yes	255	7	0.19%	0.37%
6	Yes	112	1.6	0.05%	0.04%
7	Yes	174	1	0.01%	0.03%
8	No	185	1.5	0.02%	0.69%
9	No	245	1	0.03%	0.06%

[1] Response Abbreviations: REP = pipe replacement, STR = stress relief, GWR = girth weld reinforcement, DBF = deformable backfill, INC = slope inclinometers, EHD = enhanced drainage, SST = slope stabilization, SGU = strain gages

https://doi.org/10.52202/072781-0012

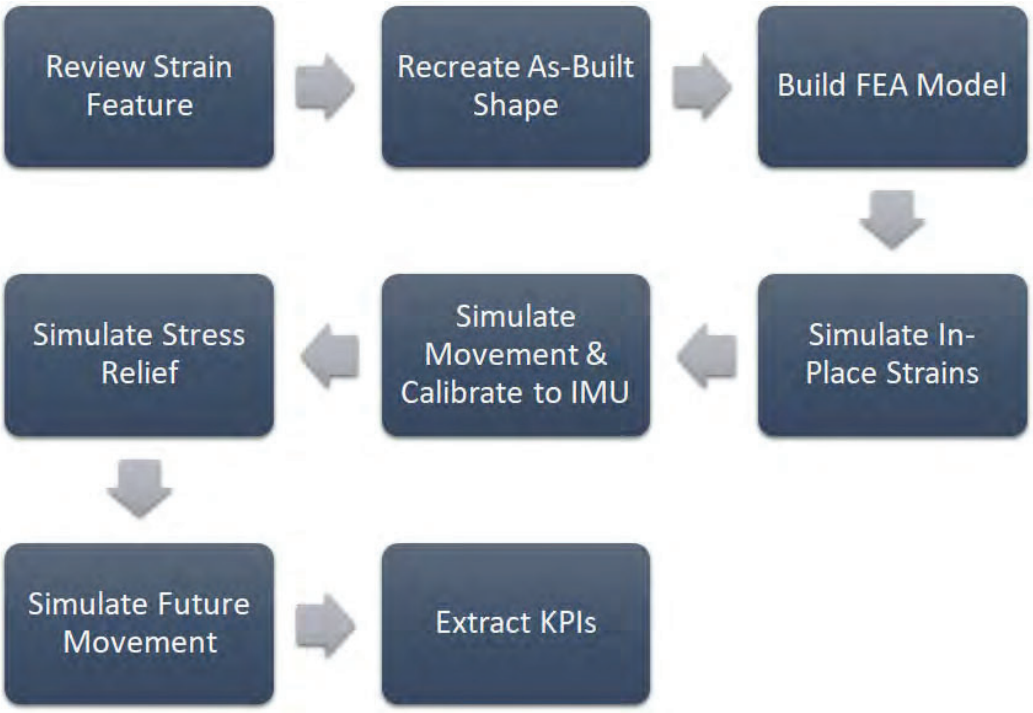

Figure 1: Analysis Process

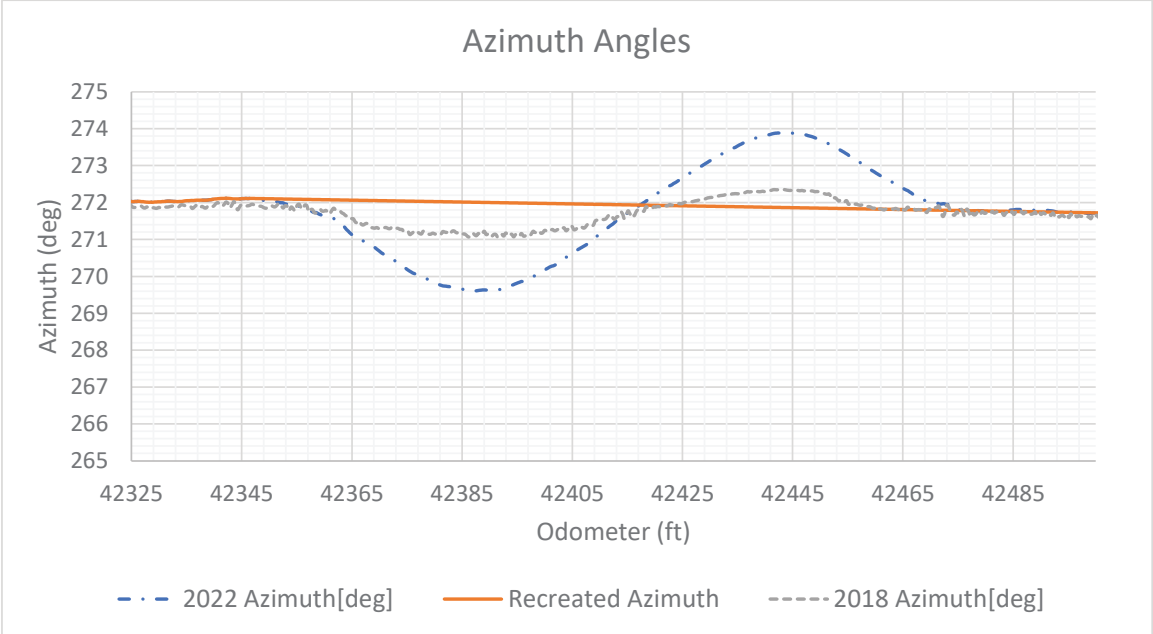

Figure 2: Azimuth Angle Recreation, Site #7

https://doi.org/10.52202/072781-0012

Figure 3: Reported Horizontal Characteristics Site #6

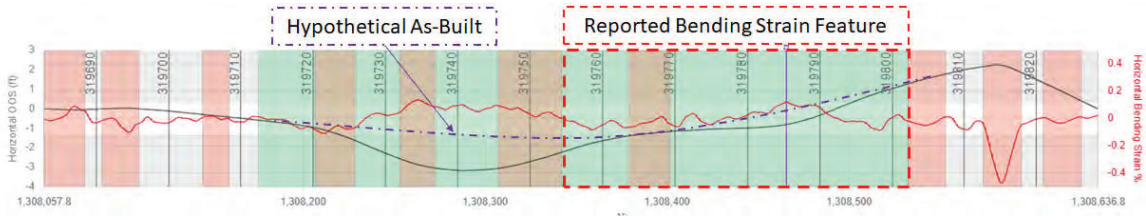

Figure 4: Site #6 Bending Strain Review with Extended Length

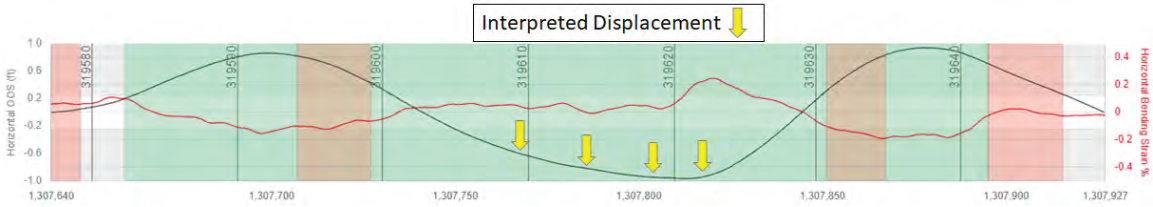

Figure 5: Reported Horizontal Characteristics Site #9

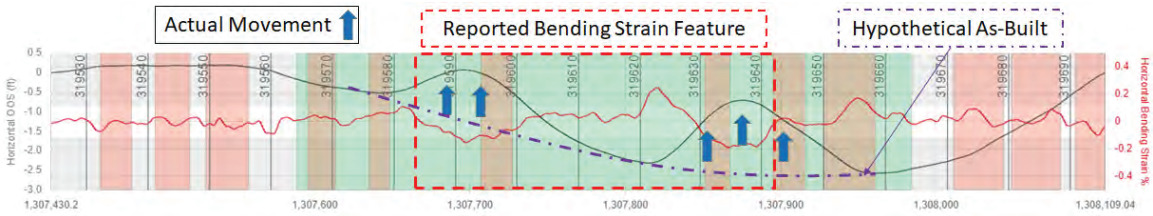

Figure 6: Site #9 Bending Strain Review with Extended Length

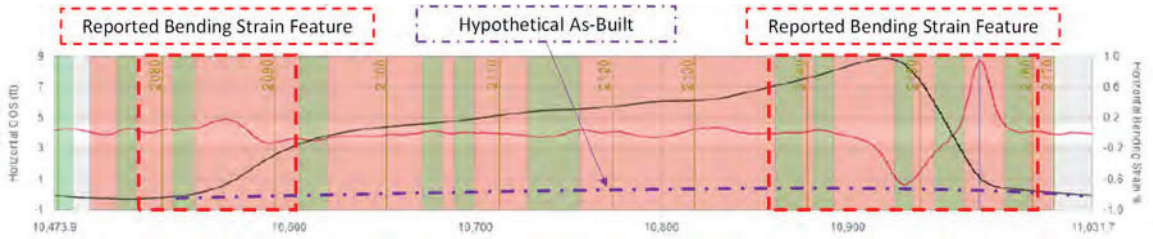

Figure 7: Site #1 Bending Strain Review with Extended Length

https://doi.org/10.52202/072781-0012

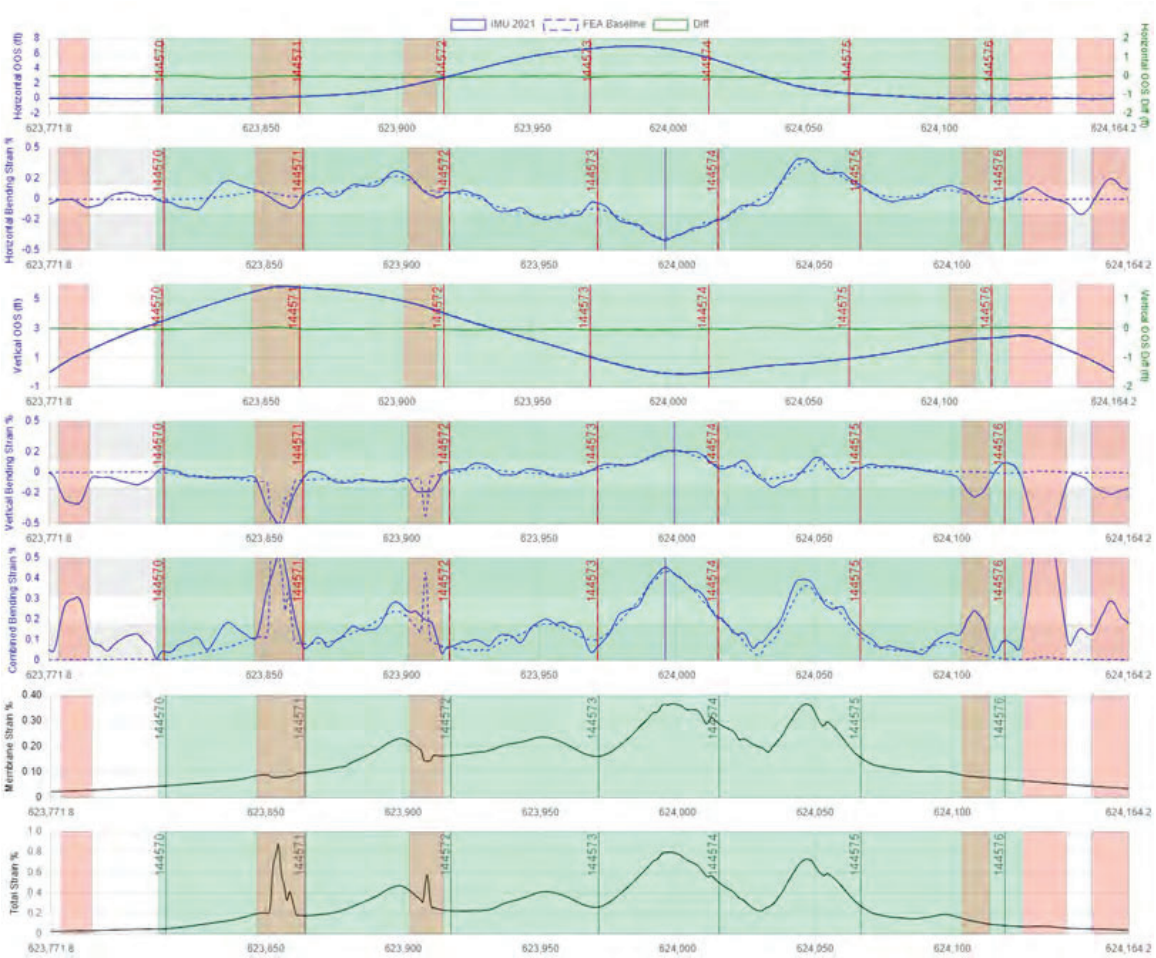

Figure 8: Site #5 Calibrated Baseline

https://doi.org/10.52202/072781-0012

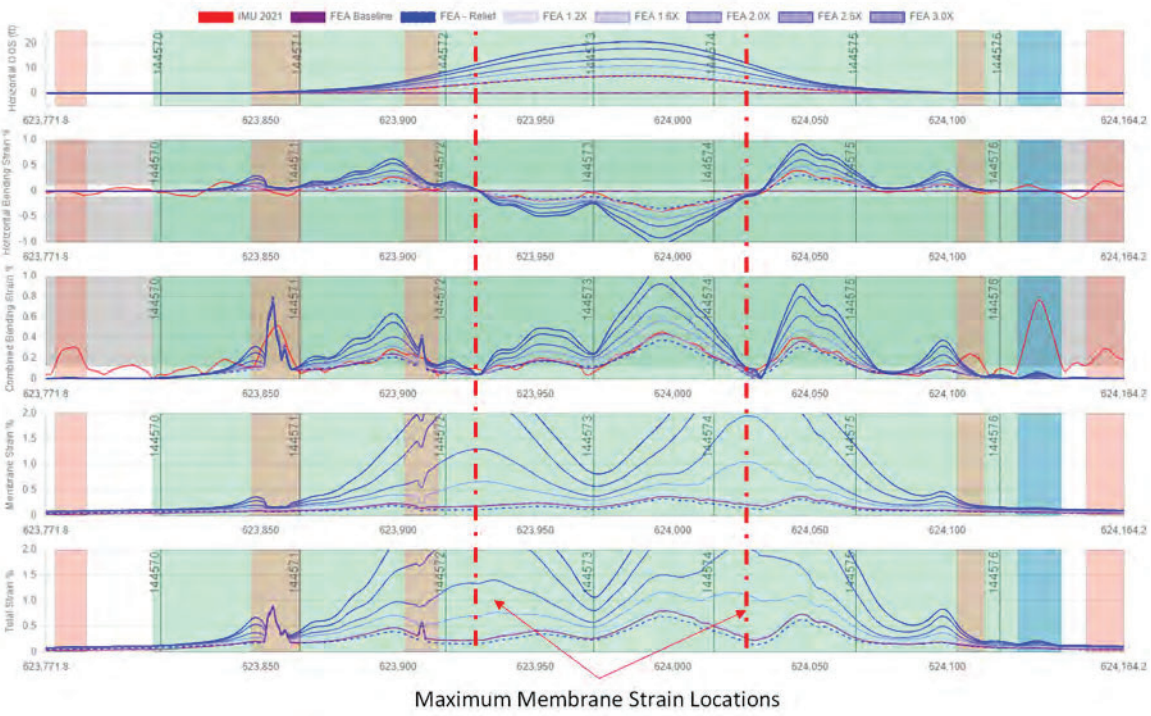

Figure 9: Site #5 Strain Profile Progression

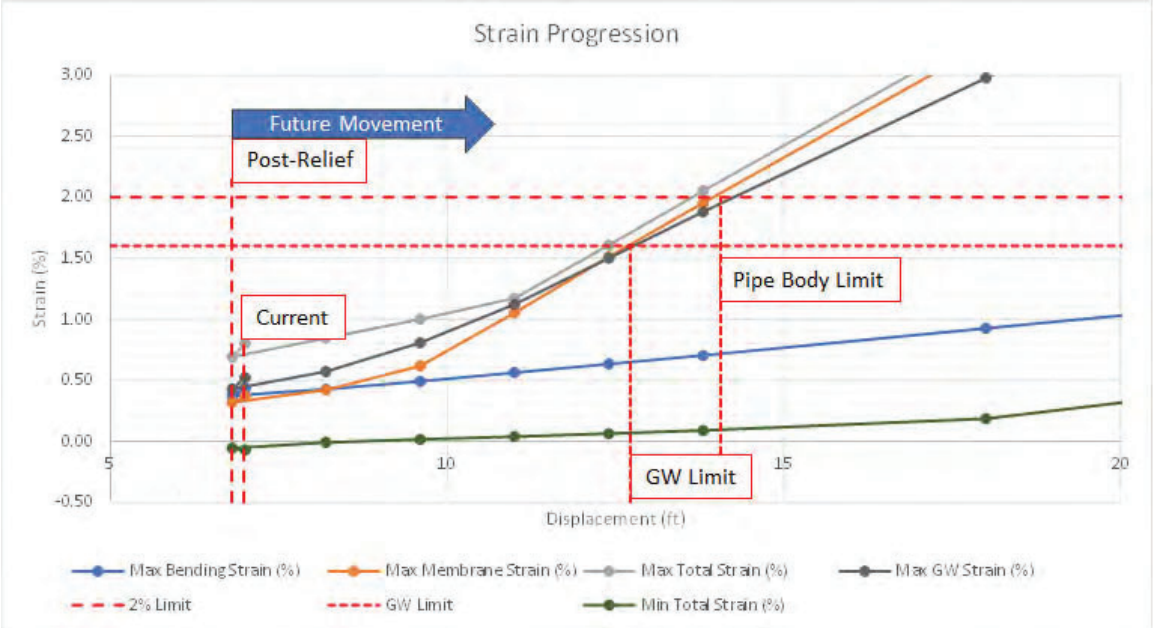

Figure 10: Site #5 Overall Strain Progression

https://doi.org/10.52202/072781-0012

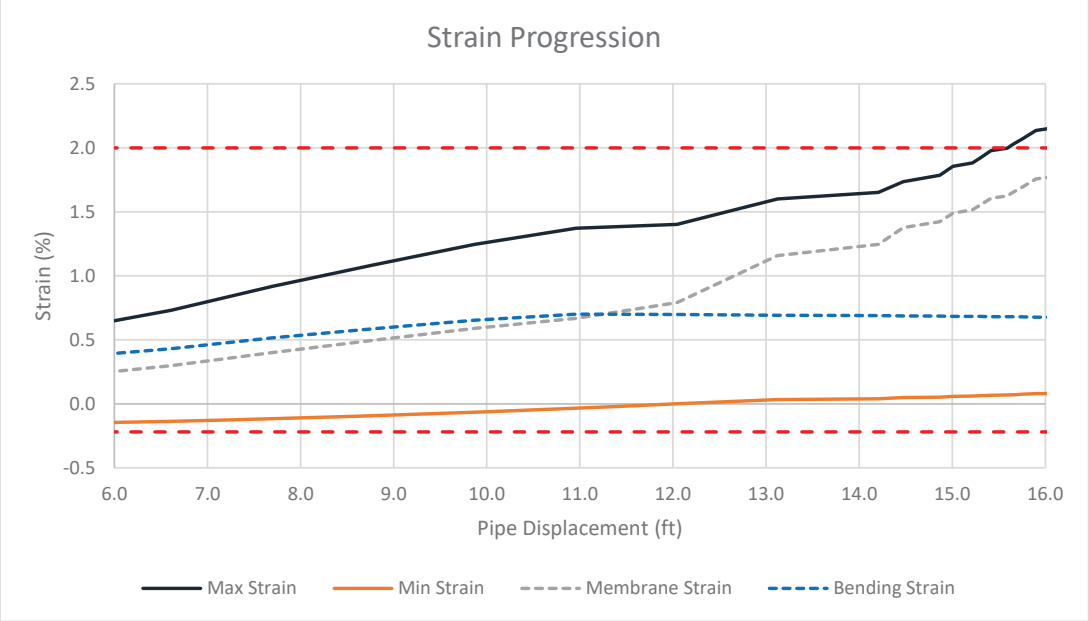

Figure 11: Site #2 Overall Strain Progression

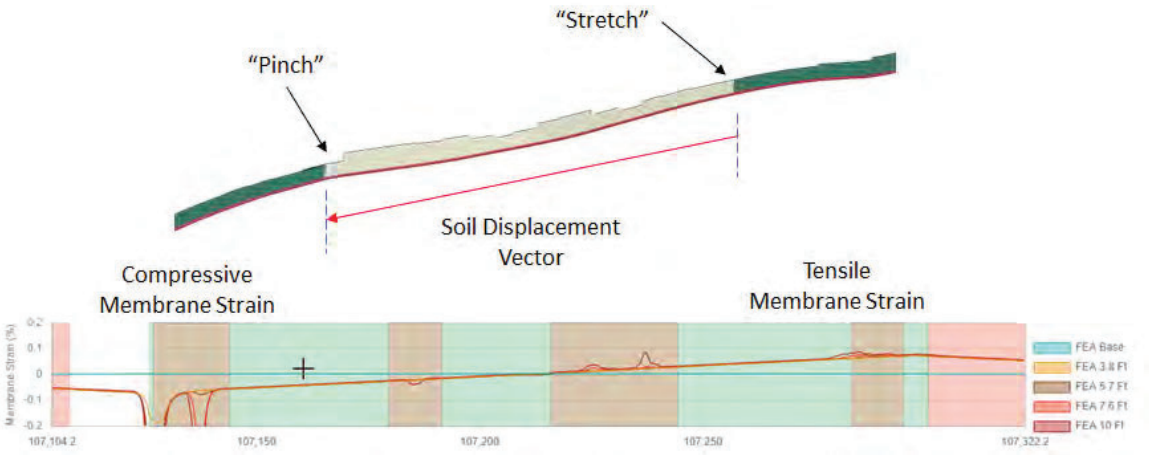

Figure 12: Site #3 Membrane Strain Progression

https://doi.org/10.52202/072781-0012

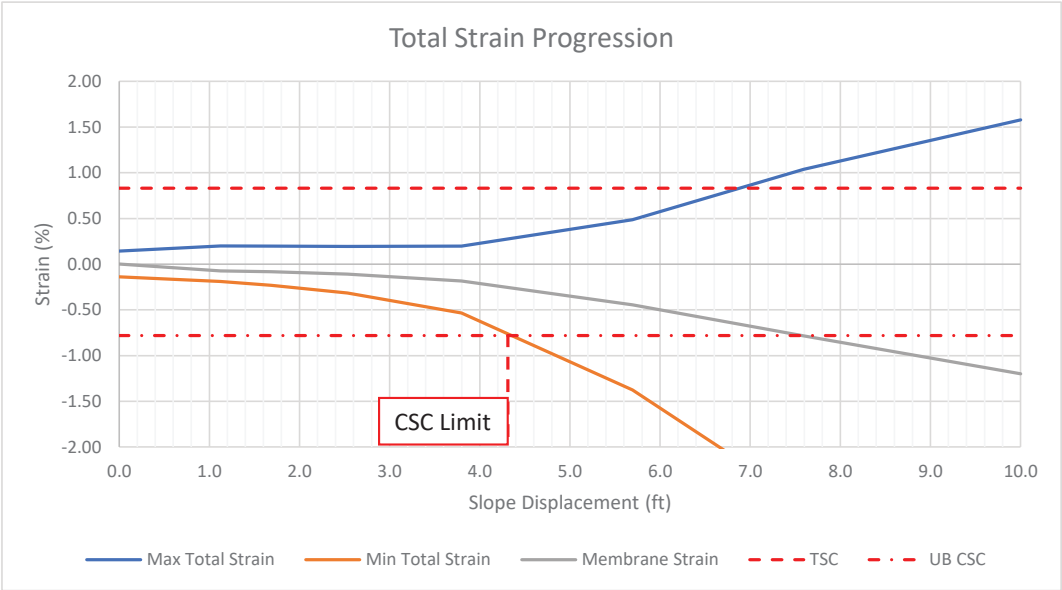

Figure 13: Site #3 Strain Progression

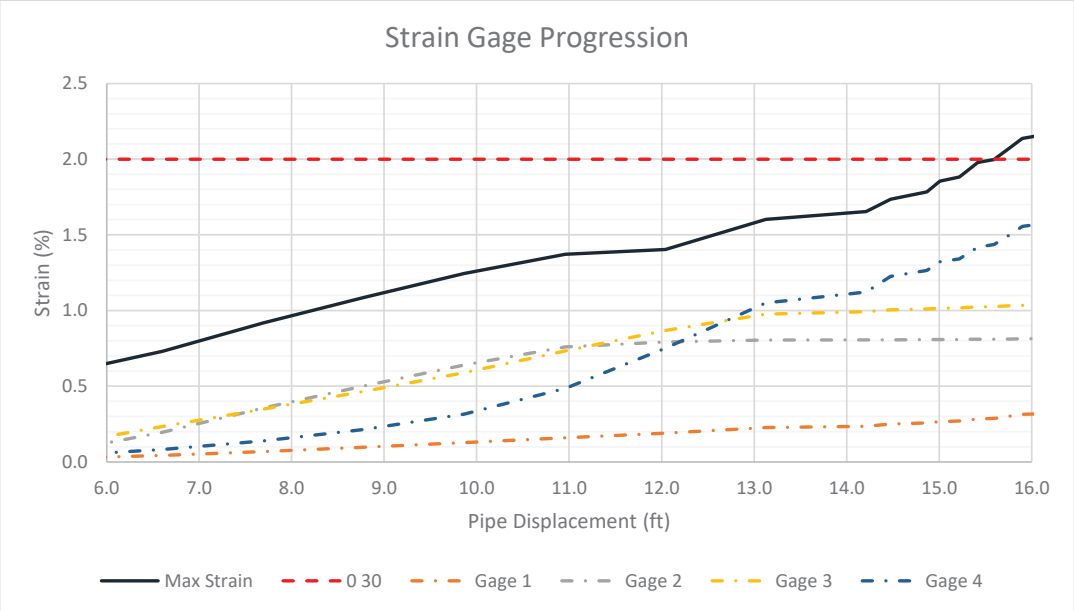

Figure 14: Site #2 Predicted Strain Gage Response

https://doi.org/10.52202/072781-0012